Research article

SJG
*Scottish Journal of Geology*

https://doi.org/10.1144/sjg2023-023 | Vol. 60 | 2024 | sjg2023-023

# A reinterpretation of the mineralization processes involved in the formation of the Tomnadashan sulfide deposit, Loch Tay, Scotland, UK

**S. Webb[1*], T. Torvela[1], R. Chapman[1], D. Selby[2] and R. Gooday[3]**

[1] Ores and Mineralisation Group, School of Earth and Environment, University of Leeds, Leeds LS2 9JT, UK
[2] Department of Earth Sciences, Durham University, Durham DH1 3LE, UK
[3] National Museums Scotland, Edinburgh EH5 1JA, UK
SW, 0000-0002-7366-7485; TT, 0000-0003-1539-8755; RG, 0000-0002-3699-1905
* Correspondence: eespdw@leeds.ac.uk

**Abstract:** The Tomnadashan sulfide deposit, which is located on the southern margin of Loch Tay (Scotland, UK), was mined for copper during the 19th century. The genetic processes at Tomnadashan remain poorly understood, and the mineralization has never been dated. To gain an improved understanding of this mineral system, we have dated the molybdenite at Tomnadashan using the Re–Os chronometer. Furthermore, we have contextualized these ages within a paragenetic interpretation. Our results show that the age of the molybdenite is *c.* 423–419 Ma, and it occurs early in the paragenesis (the second stage out of six). Based on the paragenesis of molybdenite, this age is likely to reflect the initial Caledonian mineralization event at Loch Tay. Our new data and literature review suggest that although Tomnadashan is a magmatic-related ore deposit, the porphyry that crops out is unlikely to have provided the mineralizing fluids associated with the mineralization. A concealed intrusion or granitic dykes within the porphyry may be the source of the magmatic–hydrothermal fluids. The age data indicate that the Tomnadashan mineralization is coeval with gold mineralization at Cavanacaw in Northern Ireland, giving rise to the possibility of a previously unrecognized mid-Silurian magmatic–hydrothermal episode of gold and base metal mineralization throughout the Grampian Terrane.

**Thematic collection:** This article is part of the Early Career Research collection available at: https://www.lyellcollection.org/topic/collections/early-career-research

**Received** 13 December 2023; **revised** 14 March 2024; **accepted** 20 March 2024

Around Loch Tay, which is situated in the Scottish Grampians, there are several mineral deposits with economic potential. The area south of Loch Tay is also known for historical mining of copper, lead and silver (Fig. 1; Pattrick 1984). Mining first began in the region when the Earl of Breadalbane commissioned the extraction of the aforementioned metals from the Tomnadashan sulfide deposit (herein referred to as Tomnadashan) and Coire Buidhe in the mid-19th century (Devéira 2001). The Foss Mine, a Neoproterozoic sedimentary exhalative (SEDEX) deposit, has been the site of baryte extraction since the 1970s (Moles *et al.* 2014), with further operations planned at Duntanlich in the coming years (Moles and Selby 2023). Over 1 million tonnes of baryte have been extracted from Foss (with a comparable amount yet to be mined), and at Duntanlich there is a proven resource of at least 7.5 million tonnes (MI-SWACO 2014; Moles and Selby 2023). Towards the end of the 20th century, metasediment-hosted veins around the Calliachar and Urlar burns, as well as Tombuie, were investigated for their auriferous potential by several junior exploration companies (Fig. 1; Ixer *et al.* 1997; Corkhill *et al.* 2010).

In terms of more recent exploration, since 2019, a new wave of exploration has been triggered by the discovery of high gold grades at the veins near Ardtalnaig, some of which were trialled for lead in the 19th century (https://greenglenminerals.com/project/lead-trial-prospect). However, even though the mineral deposits around Loch Tay have been known for many years, the mineralization processes and deposit models are poorly constrained. The veins, which are scattered throughout a 100 $km^2$ swathe of Dalradian metasediments, have a consistent orientation of 120–140° and are typically hosted in joints (Fig. 1). These veins are suggested to have been created during sinistral motion along the Loch Tay Fault and other similarly oriented faults at the end of the Caledonian Orogeny (Fig. 1; Corkhill *et al.* 2010). However, there are significant variations in the mineralogy and geochemistry of these veins throughout the region (Corkhill *et al.* 2010; Naden *et al.* 2010). This variation is reflected in the mineral inclusion suites preserved in alluvial gold grains, which are interpreted to indicate the presence of at least two separate mineralizing events in the wider area; one of these probably resulted from magmatic fluids (Chapman *et al.* 2022, 2023). Tomnadashan, which was not included in the study by Chapman *et al.* (2023), occurs within a composite diorite–granodiorite intrusion and is the only occurrence of mineralization around Loch Tay that has been confirmed to be directly associated with igneous activity (Pattrick 1984; Corkhill *et al.* 2010; Smith *et al.* 2022). In the context of wider comparison studies of the styles of mineralization in the Loch Tay area, it is therefore essential to better understand the mineralization at Tomnadashan.

In this paper, we present the first geochronological ages that have ever been obtained from Tomnadashan, which were

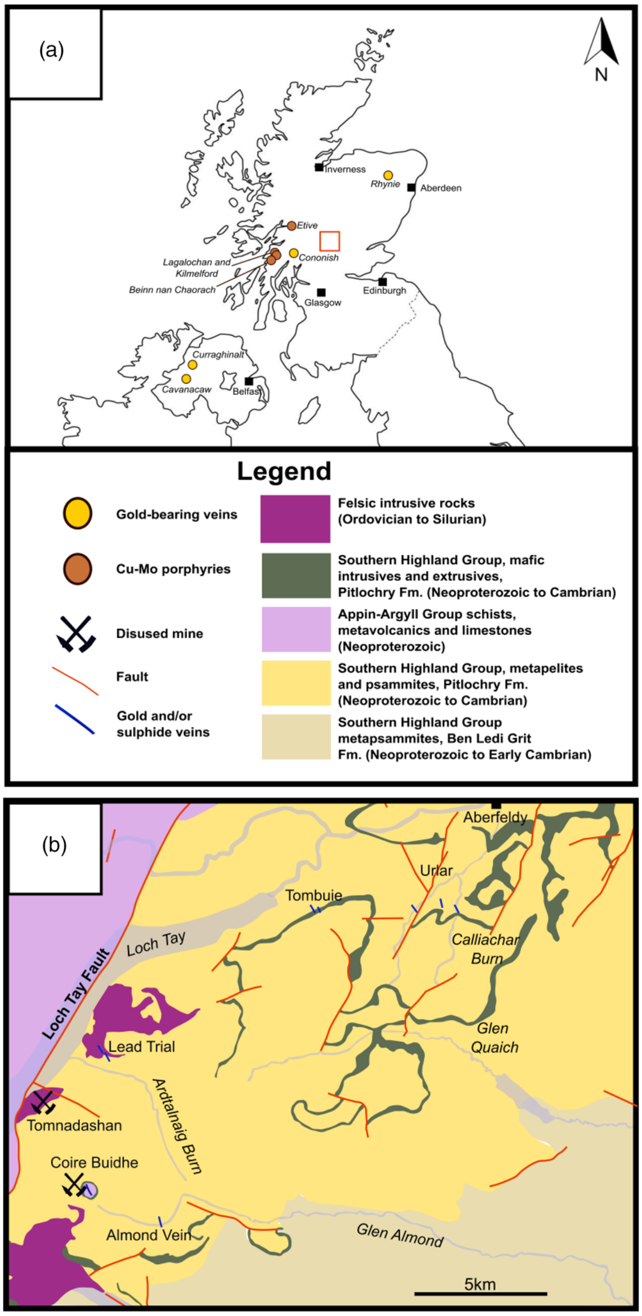


**Fig. 1.** (**a**) Location of the study area (red box) on a regional scale, annotated with occurrences of auriferous veins and Cu–Mo porphyries. (**b**) Geological map of the study area. Source: (b) adapted from Webb et al. (2024).

derived via Re–Os analyses on molybdenite. We have also undertaken a paragenetic study of the mineralization, using samples collected during fieldwork and those that are stored in the collections of National Museums Scotland (NMS) and the University of Edinburgh, to contextualize these Re–Os ages and provide further information about the style of mineralization. This information, in addition to a review of previous publications, has been used to reassess the Caledonian mineralization processes at this locality.

## Geological background

Before presenting our findings, we briefly summarize the geological evolution of the Grampian Terrane, focusing on the events around the timing of the Tomnadashan intrusion (late Silurian to Early Devonian). The Grampian Terrane largely comprises the Dalradian Supergroup, which was deposited on the Laurentian margin during the late Neoproterozoic and early Cambrian (Stephenson *et al.* 2013). The Grampian Terrane experienced deformation during the Ordovician–Silurian Caledonian Orogeny. This prolonged event resulted in the assembly of the different geological terranes into their present positions and the development of the large fault systems depicted in Figure 1a. The initial Caledonian collision (known as the Grampian phase in Scotland and Ireland) involved an approximately NW–SE convergence of Laurentia and Baltica. Crustal thickening occurred in response to thrust and nappe tectonics (Roberts and Treagus 1977; Chew and Strachan 2014; Tanner 2014*a*). The thickening stopped from *c.* 475 to 465 Ma, a temporal window often quoted as the peak metamorphic event in the Caledonian Orogeny (Friedrich *et al.* 1999; Dewey 2005; Rice *et al.* 2016). This was also accompanied by an episode of granitic magmatism (Baxter *et al.* 2002; Oliver *et al.* 2008; Mark *et al.* 2020). Several granitoid plutons in Britain and Ireland formed during this event, including the Aberdeen Granite (Oliver 2001) and the Tyrone Igneous Complex (Cooper *et al.* 2011). After the Grampian Orogeny, uplift and unroofing occurred until *c.* 430 Ma (Dempster 1985; Soper *et al.* 1999; Oliver 2001), with cooling through 300°C taking place between 460 and 430 Ma (e.g. Dempster *et al.* 1995; Soper *et al.* 1999). Generally speaking, there were a limited number of emplacement events during Iapetus subduction between 455 and 425 Ma (Oliver 2001; Oliver *et al.* 2008; Miles *et al.* 2016).

The second phase of the Caledonian Orogeny (known as the Scandian in Northern Europe) ultimately culminated in the closure of the Iapetus Ocean between 435 and 410 Ma, although the exact timing has been debated (Dewey and Mange 1999; Dallmeyer *et al.* 2001; Chew and Strachan 2014). In the Grampian Terrane, the Scandian phase caused sinistral transpressional motion along strike-slip faults (in response to roughly NW–SE-oriented stresses) sub-parallel to the structures created in the previous Grampian Orogeny (Dewey and Strachan 2003; Tanner 2014*b*). The Scandian Orogeny is related to the closure of the Iapetus Ocean, an event that included the accretion of Baltica to the Laurentian margin (Chew and Strachan 2014; Searle 2022).

Between *c.* 425 and 390 Ma, there was a widespread and long-lived episode of granitoid magmatism across the Grampian Highlands, Midland Valley and Southern Uplands of Scotland from ~425 to ~390 Ma (Jacques and Reavy 1994; Oliver *et al.* 2008; Neilson *et al.* 2009; Cooper *et al.* 2013; Hines *et al.* 2018). The specific tectonic setting regarding the emplacement of the granites at the end of the Caledonian Orogeny throughout the northern British Isles is uncertain; suggested models include a slab break-off event involving a slab of Avalonian crust that had previously been subducted beneath Laurentia (Atherton and Ghani 2002; Oliver *et al.* 2008; Miles *et al.* 2016), Avalonian slab rollback (Rice *et al.* 2018), delamination of the lithosphere (Freeman *et al.* 1988; O'Reilly *et al.* 2012), crustal extension (Dewey and Strachan 2003; Brown *et al.* 2008; Hines *et al.* 2018) and the initiation of underthrusting of the Gondwanan terranes (Miles *et al.* 2014). During the emplacement of the Newer Granites, there was a regional switch from transpression to transtension by 410 Ma, when transtensional basins were actively forming in some parts of the Scottish Grampian Terrane (Dewey and Strachan 2003).

The intrusion of the Newer Granites was possibly facilitated by the strike-slip or oblique-slip major fault systems within the Grampian Terrane (Oliver 2001). These transcurrent faults, which include the Loch Tay Fault, were initiated early during the Scandian phase, although the exact age is not known (Treagus 2003). There are no published geochronological dates for the initiation of any of these faults; however, Treagus *et al.* (1999) provided K–Ar data from the Tyndrum Fault Zone (which is similarly oriented to the Loch Tay Fault) and interpreted transtensional movement along the fault zone at *c.* 410 Ma, but by this stage the fault zone was well established.

The final event in the Caledonian Orogeny is the Acadian phase, estimated to *c*. 400–390 Ma in Scotland (Chew and Strachan 2014). The Acadian Orogeny is not particularly well-expressed in the Northern British Isles. However, some fault movement in the Grampian Terrane has yielded mid-Devonian radiometric ages, leading some to speculate that Acadian reactivation has occurred in places (Treagus *et al.* 1999; Mendum and Noble 2010).

## Geological background of Loch Tay

The Loch Tay area (the focus of this study) largely consists of the Argyll and Southern Highland Groups of the Dalradian Supergroup (Fig. 1b), locally intruded by Siluro-Devonian granitoids. Most of the mineral occurrences in the study area have a close spatial association with the Loch Tay Fault or similarly oriented structures to the south of it, or with magmatic intrusions (Fig. 1b). Treagus (2003) considered this structure to be comparable with the Tyndrum Fault, which experienced sinistral-oblique movements during the Scandian phase, at least some of which were interpreted to be transtensional (Treagus *et al.* 1999; Dewey and Strachan 2003). Dextral reactivation of the Loch Tay Fault was inferred to have occurred during the Carboniferous (Treagus 2003). Based on the geometry of the lithologies throughout the study area (i.e. some faults appear to record both sinistral and dextral displacements; Treagus 2003), it can be concluded that the Loch Tay Fault experienced reactivation at some point; however, the precise timing of this event is uncertain. Although there are many uncertainties regarding the deformational history of the Loch Tay Fault and the likely interaction between it and movements along the Highland Boundary Fault, deformation in the study area is likely to have persisted throughout the Scandian phase and into the Devonian (Chew and Strachan 2014). Some faults, including the Loch Tay Fault, cross-cut the Siluro-Devonian plutons and are therefore younger or may have experienced a post-Devonian reactivation (Treagus 2003). However, others have been interpreted to have acted as conduits for ascending plutons, and, in some cases, magmatism and faulting may have been contemporaneous (Atherton and Ghani 2002; Neilson *et al.* 2009).

## Metallogeny of the Grampian Terrane

There are several *in situ* occurrences of gold and base metal mineralization in the Grampian Terrane, some of which have a possible link with magmatic activity. Some of the occurrences are or have been mined commercially (Cavanacaw gold deposit, Northern Ireland; Cononish deposit, Scotland) or are currently being developed (Curraghinalt gold deposit, Northern Ireland; Fig. 1a). In terms of resource estimates, Curraghinalt has a measured reserve of 2.7 Moz (Rice *et al.* 2016). On the other hand, Cavanacaw has a measured reserve of at least 2 Mt at 6.9 g $t^{-1}$ Au (Parnell *et al.* 2000). At Cononish, estimated reserves are 555 000 tonnes of ore grading at 11.1 g $t^{-1}$ Au (Scotgold Resources Limited 2015).

The oldest mineralization is found at Curraghinalt, dated at *c.* 462–452 Ma (molybdenite Re–Os and sericite $^{40}Ar/^{39}Ar$ ages from gold-bearing microshears; Rice *et al.* 2016). Rice *et al.* (2016) also identified a younger, Scandian sericite $^{40}Ar/^{39}Ar$ age of *c.* 420 Ma in one of the shears, which they interpreted to reflect a reactivation of at least some of the shears at Curraghinalt; this interpretation was also advocated by Shaw (2023). There is some dispute over the genesis of Curraghinalt, with Rice *et al.* (2016) favouring an ‘orogenic’ origin over magmatic processes, whereas others have suggested a magmatic origin for the fluids (Parnell *et al.* 2000). The distinction between the two models of ore genesis stems from the fluid source; although a variety of fluid sources have been suggested for structurally controlled auriferous veins (elevated gold concentrations, low content of base metals) hosted in metamorphic belts, magmatic fluids are not the dominant fluid source (Goldfarb and Groves 2015; Goldfarb and Pitcairn 2022). Instead, most ‘orogenic’ gold deposits are interpreted as having a fluid source associated with metamorphic devolatization processes (Phillips and Powell 2010; Goldfarb and Groves 2015; Goldfarb and Pitcairn 2022). Cavanacaw was previously considered to have a genetic relationship to Curraghinalt, but a structural study by Shaw *et al.* (2022) indicated that it formed later, at *c.* 425 Ma; the nature of this deposit (magmatic v. orogenic) is still unclear.

Several gold and base metal mineralization localities are known across the Grampian Terrane in Scotland (Fig. 1a), but very few age data exist to date. Molybdenite from the Cruachan intrusion (Etive Complex) has been dated at 414.6 ± 2.1 and 414.7 ± 2.1 Ma via Re–Os methods (Porter and Selby 2010). At Cononish, *c.* 25 km SE of the Etive Complex, the auriferous mineralization has been dated at *c.* 408 Ma (K–Ar and $^{40}Ar/^{39}Ar$ ages of fault gouge and hydrothermal K-feldspar associated with the gold-bearing veins; Rice *et al.* 2012); that is, considerably younger than the gold deposits in Northern Ireland. Cononish is considered to have a genetic relationship to magmatic processes; this is further supported by the measured sulfur isotope signatures (Spence-Jones *et al.* 2018). Gold mineralization in the Rhynie Chert, NE Scotland, interpreted as an epithermal hot-spring gold deposit, shows a similar age of *c.* 407 Ma (K–Ar on alteration micas; Mark *et al.* 2011).

In the Loch Tay area, two mineralized localities are known that are related to magmatic activity. The Comrie Pluton (herein referred to as ‘Comrie’) near the Highland Boundary Fault has an alteration halo that contains some arsenopyrite mineralization (Smith *et al.* 2003). Geochronological analyses are available for Comrie, which comprises an earlier diorite phase and a later granite phase. Zircons from the granite and diorite have been dated via U–Pb laser ablation inductively coupled plasma mass spectrometry or sensitive high-resolution ion microprobe methods to 404 ± 6 and 425 ± 3 Ma respectively (based on nine zircon fractions with corrections ranging between 0.23 and 3.99%; Oliver *et al.* 2008). The second locality is Tomnadashan, which will be described in more detail in the next section.

There are several other localities south of Loch Tay with gold and base metal mineralization within quartz vein systems of variable sizes (Fig. 1b); whether these may be associated with magmatism is still under investigation by the authors. Ixer *et al.* (1997) described the 'orogenic' geochemical characteristics of fluid inclusions from the veins at the Calliachar and Urlar burns (temperatures of 320°C, 4–8 wt% NaCl, 'significant' $CO_2$ concentrations, detectable $N_2$ and $CH_4$) whereas Corkhill *et al.* (2010), based on elevated Bi concentrations throughout Loch Tay, argued that the mineralization system was genetically related to magmatism. A regional study on detrital gold from several of the localities around Loch Tay found that populations from Calliachar, Glen Almond and Glen Quaich were similar to those reported from 'orogenic' gold deposits globally, whereas samples from other streams in the southeastern part of the Loch Tay area (Fig. 1b) displayed affinities with porphyry and epithermal mineralization (Chapman *et al.* 2023).

Throughout Loch Tay, mineralized joints, and fractures, have a consistent orientation of 120–140°, or NW–SE (Corkhill *et al.* 2010). Regionally, there is broad commonality in the parageneses of the veins, in the sense that they are all composed of quartz–galena–pyrite–chalcopyrite–sphalerite mineralogies with a late input of carbonate phases (Ixer *et al.* 1997; Corkhill *et al.* 2010; Chapman *et al.* 2023; Webb *et al.* 2024). This may be indicative of coeval formation; mineralization is likely to have occurred in response to a transition from roughly north–south transpression to roughly east–west transtension (Dewey and Strachan 2003) in the Late to Post-Scandian phase. However, no geochronological studies have been done to confirm this hypothesis.

## Tomnadashan mineralization

A detailed history of the mining operations at Tomnadashan during the 19th century has been produced by Devéira (2001), who described how extraction began in 1840 and continued for 20 years, with pyritic and cupriferous ores being targeted. Small quantities of gold also occur, potentially as inclusions within the pyrite (Smith *et al.* 2003) but detailed descriptions are lacking. However, the mine was never profitable (Devéira 2001). Ore was taken by the miners to a smelter 400 m to the NW [NN 687 377] (Fig. 2a; Smith *et al.* 2022), although only 71 tonnes of saleable copper and sulfur ores were ever produced (McKerracher 1988; Smith 1996). Geologically, the Tomnadashan deposit is hosted within a porphyry adjacent to the Loch Tay Fault (Fig. 1b). This porphyry comprises different compositional zones, with diorite, granodiorite and granitic subdivisions being recognized (Fig. 2a and b; Pattrick 1984). The granitic zones have been affected by potassic alteration, with patches of propylitic alteration occurring throughout the other lithologies (Smith 1996); Pattrick (1984) described the Tomnadashan mineralization as

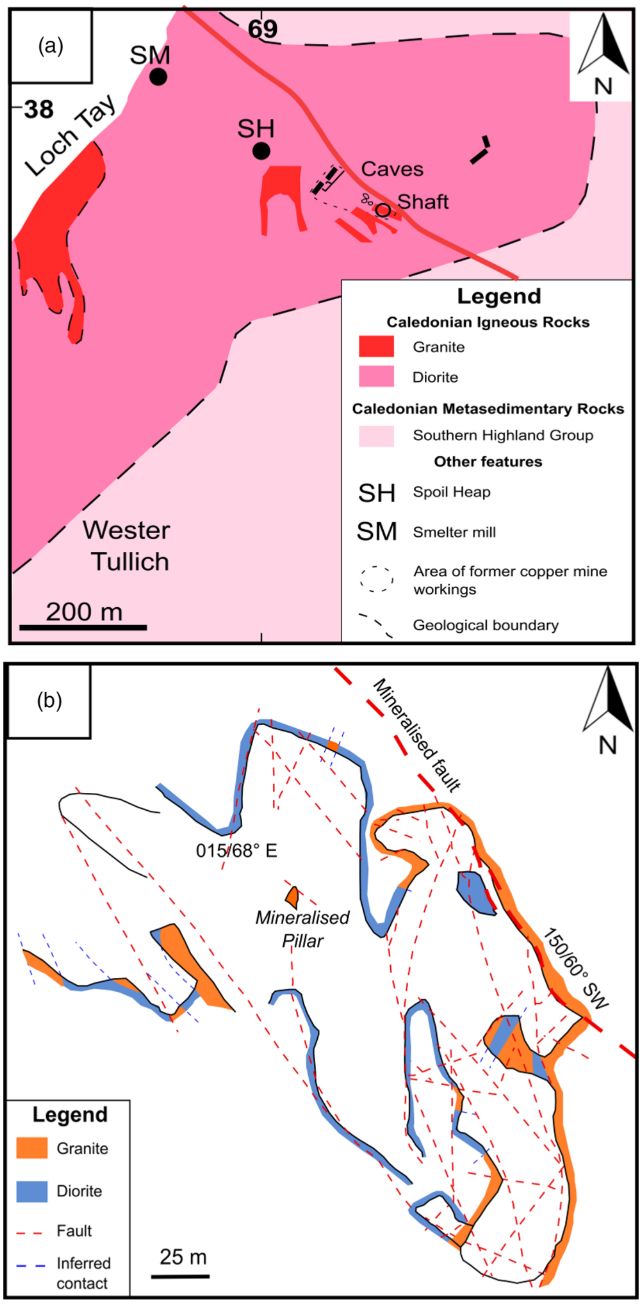


**Fig. 2.** (**a**) Geological map of the Tomnadashan pluton. (**b**) Geological map of the mine workings. Sources: (a) adapted from Smith *et al.* (2022); (b) adapted from Smith (1996).

belonging to a 'porphyry' style of mineralization. Historical records of extraction noted how two 15–100 cm wide lodes that trend east–west and NW–SE were mined at Tomnadashan (Henwood 1871), with the latter hosting the mineralization (Halliday 1961). Tomnadashan is distinct from the vein-hosted localities in the sense that the gold and silver contents appear to be considerably lower (2.2 ppm Au and 34 ppm Ag; Smith *et al.* 2022), although precious metal mineralization is evidently still present. Mineralization is focused along the faulted contact between the diorite and granodiorite (Fig. 2b), with the intensity waning with distance from this geological boundary (Naden *et al.* 2010). However, beyond these previously mentioned descriptions on the distribution of the mineralization at Tomnadashan, there is little constraint on the extent of mineralization within the porphyry; other parts of the mine (e.g. the 'Mineralised Pillar' in Fig. 2b) record mineralization and Smith (1996) noted the occurrence of quartz veinlets within the dioritic portions of the pluton. The previously published descriptions of the Tomnadashan mineralization clearly indicate that the porphyry that crops out at the surface is simply the host rock of the ore deposit; it is possible that mineralizing fluids were sourced from the granitic dykes within the mine (Fig. 2b) or a concealed porphyry at depth (potentially along the Loch Tay Fault; Fig. 1b). The actual 'Tomnadashan sulfide deposit' is a NW–SE-trending fault-hosted quartz ± carbonate vein, with the granitoid host rock containing some disseminated mineralization, possibly related to this veining event.

Approximately 19 mineral species have been recognized at Tomnadashan (Smith *et al.* 2022), with the paragenesis being subdivided into two stages (Pattrick 1984; Smith *et al.* 2022) as follows: (1) pyrite + molybdenite + bismuthinite inclusions, tennantite, aikinite ($PbCuBiS_3$) and hodrushite ($Cu_8Bi_{12}S_{22}$); (2) chalcopyrite + galena + native bismuth + tetrahedrite.

The paragenesis produced by Pattrick (1984) provides no SEM or petrographic images to support the paragenetic interpretation. Furthermore, that publication did not provide any information on whether the samples used in the paragenetic interpretation came from the disseminated mineralization in the granitoid or the mineralized quartz ± carbonate vein. Although Pattrick (1984) did not observe gold at Tomnadashan, Smith *et al.* (2003) described it as an included microscopic phase within the pyrite, potentially implying that it is part of the first paragenetic stage.

Moorbath (1962) sought to calculate the age of mineralization at Tomnadashan using Pb isotopes. However, the Holmes (1946) model of Pb evolution was relied upon in this calculation; this model is now known to yield inaccurate ages (Huston and Champion 2023). Although the age this analysis yielded (530 ± 60 Ma) is likely to be incorrect (it would place the formation of Tomnadashan prior to the existence of the orogenic belt, which it cross-cuts), the Moorbath (1962) study provided $^{206}Pb/^{204}Pb$ and $^{207}Pb/^{204}Pb$ isotope ratios of 17.6 and 15.3, respectively. These values would plot beneath the 'plumbotectonics' lead growth curve for the mantle by Zartman and Doe (1981), potentially indicating that this is the ultimate source of Pb for the deposit. Some limited $\delta^{34}S$ work has also been done on pyrite from Tomnadashan (+0.5 and +2.0‰ for the granite and diorite respectively) (Lowry *et al.* 2005). These values were considered to reflect the trend observed in wider $\delta^{34}S$ studies from the Grampian Terrane, in which the 'Newer Granites' contain disseminated sulfide with $\delta^{34}S$ values of −3‰ to +3‰ (Lowry *et al.* 2005). This regional signature was interpreted to reflect a 'subcrustal magmatic' source of sulfur, with minimal modification to the $\delta^{34}S$ of the sulfides resulting from rapid ascent and cooling, as well as a relatively hot (>400°C) precipitation environment (Lowry *et al.* 2005). Furthermore, previous fluid inclusion studies of Tomnadashan (Naden *et al.* 2010) have identified broad similarities to fluid inclusion populations from porphyry Cu–Mo deposits (NaCl > 35 wt%, homogenization temperatures >300°C; Sillitoe 2000).

In the present study, we have sought to contribute towards understanding the metallogeny in the Loch Tay area by investigating the paragenesis and the age of the Tomnadashan sulfide mineralization. In addition to constraining the age of the mineralization in the area, the obtained age data illuminate the regional evolution of the late Caledonian magmatic system.

## Methods

The samples and mineralogical and textural observations are summarized below before describing the molybdenite Re–Os age dating (the samples utilized in these analyses are depicted in Fig. 3).

### Mineralogical mapping

To contextualize the age data and refine the published paragenetic interpretations, a paragenetic study on the Tomnadashan mineralization (Fig. 4) was conducted using the principles outlined by Webb *et al.* (2024). Ten polished blocks and five thin sections, covering both the disseminated and vein-hosted aspects of the mineralization (Fig. 4), were utilized in this process. The samples were collected from the spoil tips (Fig. 2a, 'SH') immediately outside the mine (e.g. the samples shown in Fig. 4) and although it is known that they were originally extracted from the underground Tomnadashan mine workings (Devéria 2001) their exact

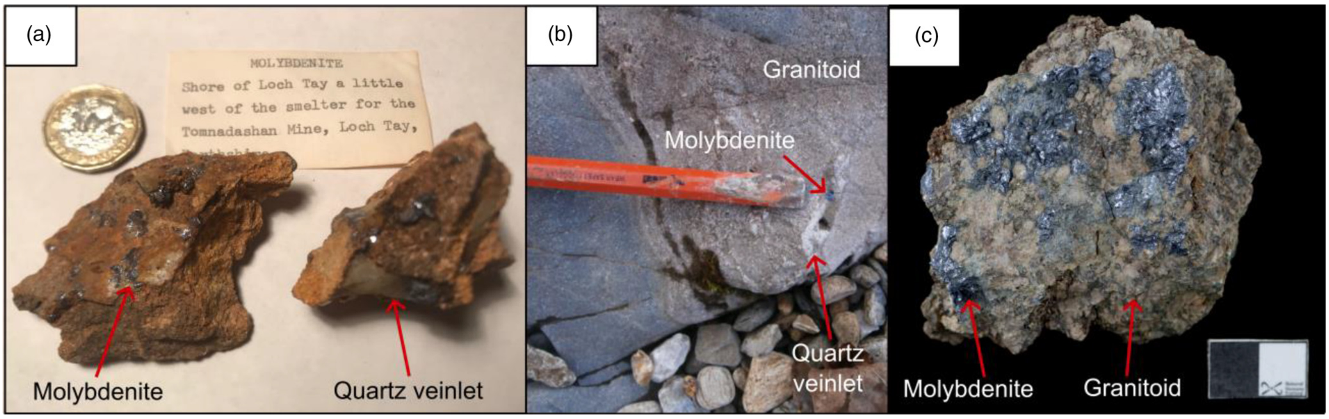


**Fig. 3.** Samples of molybdenite at Tomnadashan that were dated via the Re–Os chronometer. (**a**) TOM_MOLY_SM (quartz vein-hosted molybdenite). (**b**) PA_MOLY (quartz vein-hosted molybdenite). (**c**) G.1878.49.10.1 (molybdenite disseminated in the granitoid host rock with pyrite). Source: © National Museums Scotland.

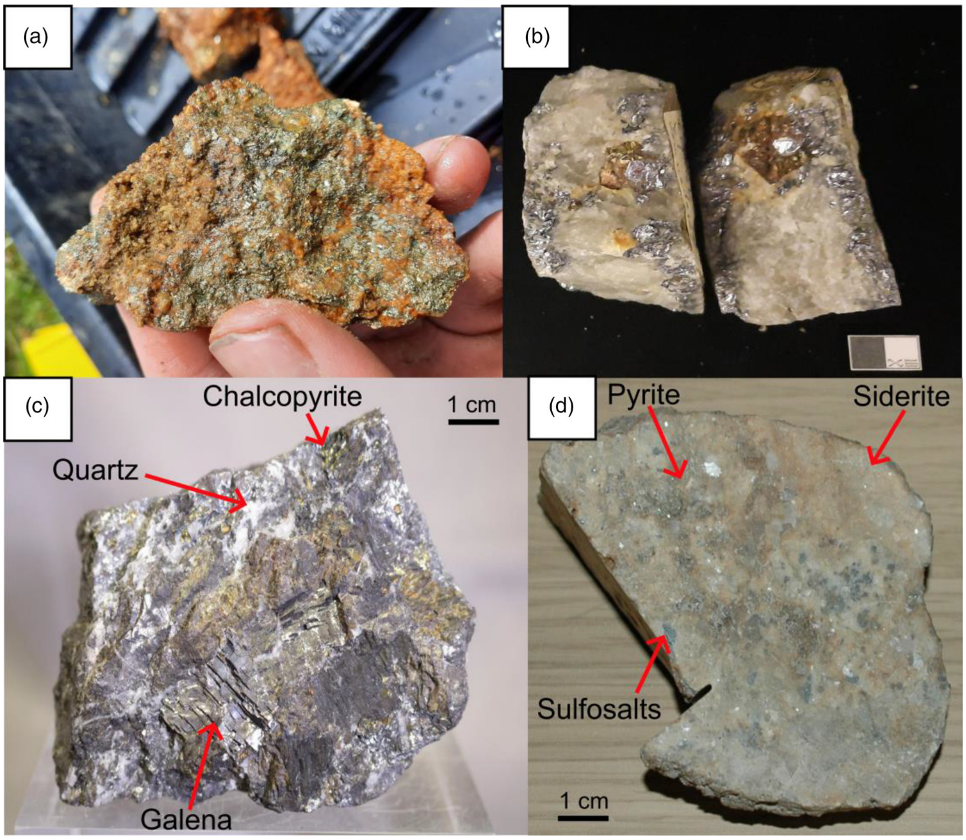


**Fig. 4.** Examples of the typical mineralization at Tomnadashan, some of which were used to create polished blocks and thin sections utilized in the paragenetic interpretation. (**a**) SW_TOM_PY; fine-grained (<2 mm) disseminated pyrite mineralization within the granite host rock. (**b**) 1908.22.1.1 + 1.2; coarse-grained molybdenite growing along the contact between the granitoid and quartz vein. (**c**) G.2019.101.7; massive to platy sphalerite associated with chalcopyrite and galena. (**d**) TOM_QTZ; pyrite and sulfosalts growing in the quartz ± carbonate vein. Sources: (b) and (c) © National Museums Scotland.

*in situ* provenance remains unknown. The mineralogical and textural mapping was conducted using a Tescan VEGA3 XM SEM with a back-scattered electron (BSE) detector facility, allowing micron-scale, semi-quantitative compositional analysis of the phases in the samples. We focused on using the law of cross-cutting relationships to establish the paragenetic order of the different phases, as this is the most powerful tool used in paragenetic studies owing to the lack of ambiguity in interpretation relative to other paragenetic criteria (Webb *et al.* 2024). However, the relatively small scale of our study means that it has not been possible to observe cross-cutting relations between all phases; other paragenetic indicators have been used where appropriate but this is a common limitation when scrutinizing the paragenesis of orebodies, which can be several kilometres long.

## Age determinations

For Re–Os age determinations, two samples of molybdenite (TOM_MOLY_SM and PA_MOLY; Fig. 3a and b) were collected from the smelter mill situated close to the Loch Tay shoreline, and a third sample from the mine itself was sourced from the National Museums Scotland collection (G.1878.49.10.1; Fig. 3c). Mineralogically, sample G.1878.49.10.1 is mostly composed of very fine-grained (1 mm) molybdenite crystals and fine-grained pyrite. Fine-grained molybdenite is particularly important for Re–Os date determination as previous research has demonstrated that any post-mineralization decoupling of Re and $^{187}$Os is easier to overcome via sample homogenization in a mineral separate and aliquant analysis, and hence this approach is more likely to yield precise and accurate ages (Stein *et al.*, 2001; Selby and Creaser, 2004; Selby *et al.*, 2004; Porter and Selby, 2010). TOM_MOLY_SM and PA_MOLY comprise quartz veinlets cross-cutting the granitoid host rock and bringing in coarse, euhedral molybdenite flakes (<5 mm in size, typically between 2 and 4 mm; Fig. 3a and b). The historical records clearly show that the smelter was used by the artisanal miners to dump *in situ* material removed from the mine (Devéira 2001).

Molybdenite mineral separates and Re–Os analysis were obtained at Durham University in the Durham Geochemistry Centre. Fractions of the molybdenite samples were individually crushed, using an agate pestle, to 10 mesh (~2 mm) and then handpicked under a binocular microscope to remove non-molybdenite phases. The separated and picked molybdenite fractions were loaded into Teflon beakers with 10 ml 32N HF at room temperature overnight to dissolve any quartz remaining in the fraction (Lawley and Selby 2012). The molybdenite crystals were then rinsed with Milli-Q water (MQ) three times and further rinsed with ethanol, and then dried at ~35°C. The molybdenite aliquots were further purified by hand under a binocular microscope to remove any pyrite, chalcopyrite and undissolved silicate phases. The Re–Os analytical protocol utilized an established procedure (Li *et al.* 2017). In brief, a known amount of molybdenite (typically >20 mg) and tracer solution ($^{185}$Re and isotopically normal Os; Selby and Creaser 2001) was loaded into a Carius tube (Shirey and Walker 1995) with 3 ml 15.5N HCl and 6 ml 16N $HNO_3$, sealed and placed in steel jackets, and then heated to 220°C in an oven for *c.* 24 h to permit isotope equilibration of both rhenium and osmium between the tracer solution and sample (Selby and Creaser 2001). The Os was isolated from the acid medium using a solvent extraction ($CHCl_3$) and then back extracted into HBr and further purified by microdistillation. Rhenium from the Os extracted acid medium was obtained by NaOH–acetone solvent extraction and further purified via anion chromatography.

The isotopic compositions of Re and Os were measured using static Faraday cups collection by negative thermal ionization mass spectrometry (N-TIMS) on Ni and Pt filaments, respectively (Creaser *et al.* 1991; Völkening *et al.* 1991) using a Thermo Scientific Triton mass spectrometer. The measured Re and Os isotope compositions were corrected using an $^{18}O/^{16}O$ and $^{17}O/^{16}O$ value of 0.002045 and 0.001113 (Nier 1950). The isotopic composition of Re was corrected for instrumental fractionation by fractionation factors defined by the differences between standard Re analyses and the value of Gramlich *et al.* (1973) ($^{185}Re/^{187}Re = 0.59738$). The Os mass fractionation was monitored in real time by monitoring the Os isotope composition of the tracer and corrected using an $^{192}Os/^{188}Os$ value of 3.08761. The uncertainties of sample Re and Os isotope composition measurements, tracer calibration, sample and tracer weighting, reproducibility of Re and Os isotope standards, as well as blank abundances and isotopic compositions during the course of study were all propagated. During this study, the Re and Os blanks were 2 and 0.5 pg, respectively, with an $^{187}Os/^{188}Os$ value of 0.24 ± 0.01 ($n = 6$, 2σ). The molybdenite Re–Os model age was calculated using the equation $t = \ln(^{187}Os/^{187}Re + 1)/\lambda$, in which $\lambda$ is the decay constant (Smoliar *et al.* 1996).

## Results

The observations and relationships in the analysed samples are described in Table 1 and shown in Figure 5. Key observations most relevant to this study are summarized briefly below. According to the convention for describing paragenetic relations outlined by Webb *et al.* (2024), each stage is given a number depending on order. However, when a phase occurs repeatedly throughout the paragenesis, it may be given an alphabetical identifier (A–Z), in addition to the Warr (2021) abbreviation, for extra clarity. For example, pyrite from Stage 1 is referred to as 'PyA', whereas pyrite from Stage 3 is termed 'PyC' (Table 1; Fig. 5g). The reasoning behind this convention is that it makes annotating petrographic images easier; for example, annotating the pyrite with 'PyA' in Figure 5a is easier than having to write 'Stage 1 Pyrite'.

Pyrite occurs in two distinct styles: one (PyA) with inclusions of bismuth tellurides (Fig. 5d), intergrowing with chalcopyrite (CcpA; Fig. 5e) and another (PyC) with inclusions of galena and tennantite–tetrahedrite (Fig. 5g and h). Molybdenite is seen to occur within at least PyA where it occupies elongate features, possibly fractures, within PyA (Fig. 5b). Tennantite and tetrahedrite were observed as coeval inclusions within PyC (Fig. 5g) and may form a solid solution series with one another (TntC and TtrC; Fig. 5h). Sphalerite occurs together with galena, enveloping fragments of CcpA (Fig. 5i). Late quartz veins with chalcopyrite cross-cut earlier phases (Fig. 5j); similarly, late tetrahedrite veinlets (TtrD; Fig. 5f) cross-cut the sulfosalts that formed earlier. Finally, carbonate phases (Fig. 5k and l) cross-cut other phases; however, we have not been able to directly observe the relationships of the siderite to the sulfide phases in thin section.

### Age determinations

The results of the dating are summarized in Table 2. The samples all contained abundant Re (123.5 ppm for TOM_MOLY_SM; 209.9 ppm for G.1878.49.10.1; 106.1 ppm for PA_MOLY) and $^{187}Os$ (548.3 ppb for TOM_MOLY_SM; 924.0 ppb for G.1878.49.10.1; 471.6 ppb for PA_MOLY). The obtained dates range from 419 ± 2.1 to 423 ± 2.2 Ma. The results are mutually consistent with low uncertainty margins (*c.* 0.5% uncertainty), supporting negligible uncertainties and errors in the procedure and homogeneity within the analysed molybdenite crystals.

## Interpretation

### Paragenesis of the Tomnadashan deposit

The petrographic characterization of the Tomnadashan samples provides the context for the molybdenite Re–Os data and has revealed a multistage paragenesis (Fig. 6). The molybdenite dated in this study occurs in the second stage (Fig. 6; Table 1), which has been overprinted by an episode of pyrite, galena, sphalerite and copper sulfosalts. This was followed by a late stage of quartz, chalcopyrite and tetrahedrite veinlet injection (Fig. 6; Stage 4), followed by the precipitation of carbonate minerals (Fig. 6; Stages 5 and 6). No differences in the paragenetic sequences recorded by the disseminated and vein-hosted mineralization could be observed.

Apart from the context of the dated molybdenite, we can refine the previously published paragenetic interpretations (which have also been incorporated into Fig. 6). By and large, there are similarities to the paragenetic interpretations provided by Pattrick (1984) and Smith *et al.* (2003), but our SEM data allow the construction of a more detailed interpretation. The paragenetic relationship between PyA and PyC is supported by the tendency for sulfosalt veinlets to cross-cut PyA but not PyC (Fig. 5f). Furthermore, tetrahedrite can be observed to cross-cut the tennantite (Fig. 5f). The sulfosalts themselves are cross-cut by small veinlets containing quartz and chalcopyrite (Fig. 5j). In terms of the final paragenetic stages of the orebody, these are devoid of sulfide mineralization. Stage 5 contains voluminous siderite precipitation (Fig. 5a), accompanied by the precipitation of hydrothermal monazite (Fig. 5k). The last paragenetic stage contains baryte (Fig. 5b and k) and dolomite veinlets (Fig. 5l).

However, as noted by Webb *et al.* (2024), a limitation in any paragenetic study is the ability to study a quantity of material that is representative of the orebody. This may explain why the gold inclusions in the pyrite described by others (Smith *et al.* 2003) could not be observed during our study (Table 1). However, gold has been panned from the stream flowing out of the entrance to the Tomnadashan Mine; the microchemical signature of these particles is being characterized as part of a current study, although an inclusion of wittichenite (a copper bismuth sulfide) has been found so far (Fig. 5c). This potentially indicates that gold occurs in Stage 1 of the paragenesis (alongside the bismuth tellurides, although this is uncertain, as indicated in the final paragenetic interpretation; Fig. 6).

**Table 1.** Observations made during textural mapping, with references to representative SEM and reflected light microscopy (RLM) images from Tomnadashan

| Mineral | Thin section(s) ID | A | B | C | D | E | F |
|---|---|---|---|---|---|---|---|
| Quartz | TOM_QTZ; TD-0 (vein) | QzA-C; Indistinguishable CL response. Featureless subhedral Qz crystals in the quartz vein, sometimes growing alongside Py (Fig. 5a) | | | Hairline fractures cross-cutting sulfides or sulfosalts (Fig. 5b and j) | | |
| Pyrite | SW_TOM_PYa + b (disseminated), TOM_QTZ (vein) | PyA; <1 cm crystals with inclusions of Mol and Bi tellurides (Fig. 5b–d); cross-cut by Ttr (5f) | | PyC; contains inclusions of Gn, Tnt and Ttr (Fig. 5g and h) | | | |
| Bi tellurides | SW_TOM_PYa (disseminated) | Inclusions within PyA (Fig. 5d) | | | | | |
| Chalcopyrite | SW_TOM_PYa + b (disseminated), TOM_QTZ, B0018 (vein) | CcpA; intergrows with PyA (Fig. 5e) | | | CcpD; late-stage veinlets cross-cutting Ttr (Fig. 5j) | | |
| Molybdenite | B003 (disseminated) | | Inclusions within PyA (Fig. 5b) | | | | |
| Galena | TOM_QTZ, B0018 (vein) | | | GnC; voluminous stage (Fig. 4c); brecciates CcpA (Fig. 5i); GnC also occurs as coeval inclusions in PyC (Fig. 5g) | | | |
| Sphalerite | B0018 (vein) | | | SpC coprecipitates with GnC in Figure 5i | | | |
| Tetrahedrite | TOM_QTZ (vein) | | | TtrC occurs as inclusions within PyC (Fig. 5h) | TtrD cross-cuts PyA and TntC (Fig. 5f) | | |
| Tennantite | TOM_QTZ (vein) | | | TntC occurs as inclusions within PyC (Fig. 5g); envelops PyA; may form solid solution series with TtrC (Fig. 5f and h) | | | |
| Monazite | TOM_QTZ (vein) | | | | | Intergrows with voluminous Sd (Fig. 5k) | |
| Siderite | TOM_QTZ (vein) | | | | | Fe-bearing, zoned (Fig. 5a); coprecipitates with Mnz (Fig. 5k) | |
| Dolomite | TOM_QTZ (vein) | | | | | | Veinlets cross-cutting or replacing Sd (Fig. 5l) |
| Baryte | TOM_QTZ (vein) | | | | | | Veinlets cross-cutting all phases (Fig. 5b and k) |

A–F represent the relative order of the different minerals. The terms ‘disseminated’ and ‘vein’ are used to demonstrate the origin of the samples. In the Thin Section ID column, the parentheses after each sample indicate whether the mineralization is disseminated in the granitoid or hosted in the vein.

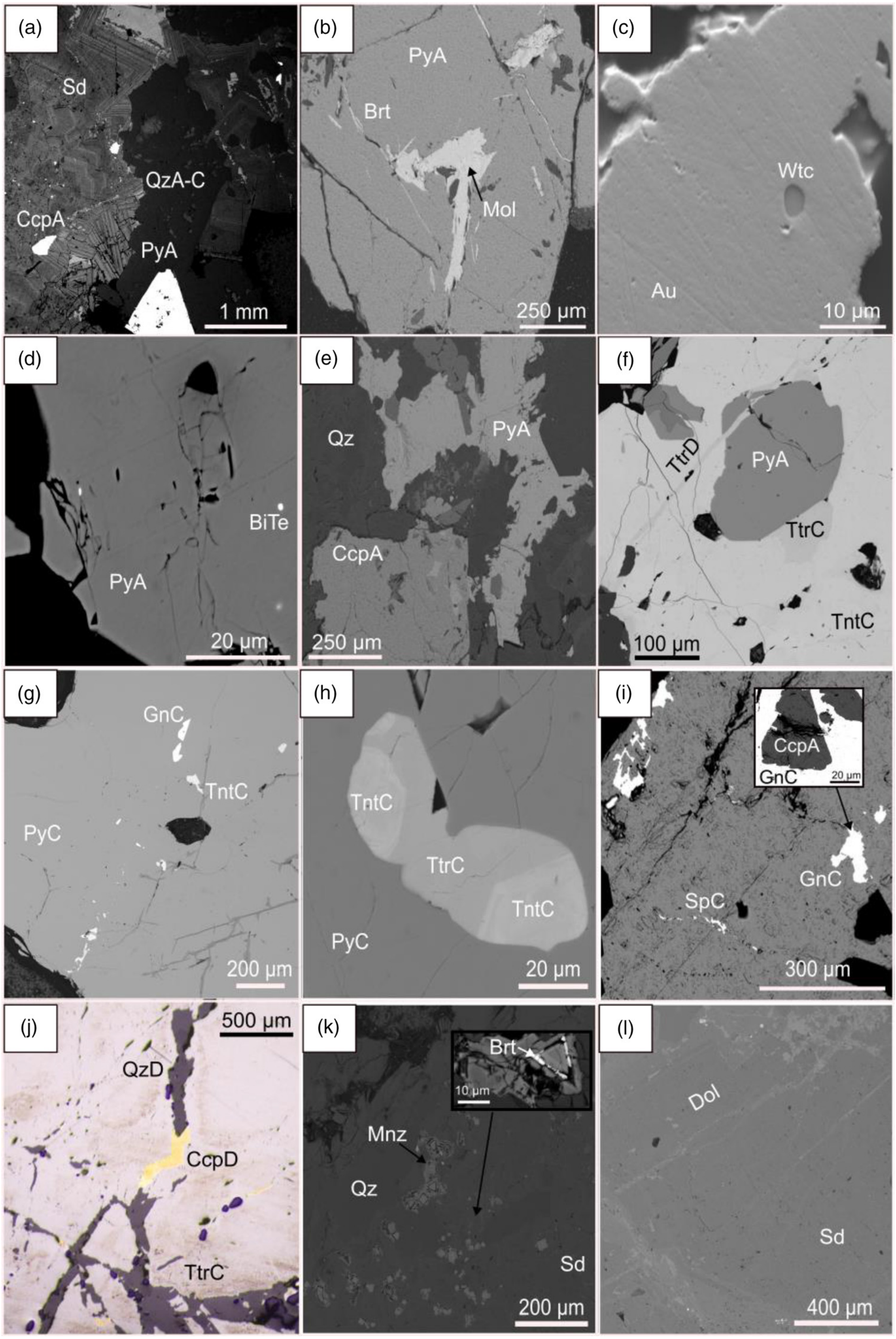


**Fig. 5.** BSE and RLM images of representative vein textures illustrating the relationships described in Table 2. (**a**) Siderite cross-cutting quartz. (**b**) Molybdenite precipitating in PyA fractures. (**c**) Gold particle (containing a coeval wittichenite inclusion) that was recovered from the stream flowing out of the Tomnadashan Mine. (**d**) Coeval BiTe inclusions within PyA. (**e**) CcpA growing alongside PyA. (**f**) Copper sulfosalt veinlets cross-cutting PyA; Ttr and Tnt are interpreted to form a coeval solid solution here. (**g**, **h**) Galena, and copper sulfosalts demonstrating a solid solution series, occurring as coeval inclusions within PyC. (**i**) Galena inclusions precipitating within sphalerite. (**j**) RLM image showing veinlets containing QzD and CcpD cross-cutting tetrahedrite. (**k**) Baryte infilling monazite that is coeval with the siderite. (**l**) Late-stage dolomite veinlets cross-cutting or replacing the siderite. Qz, quartz; Py, pyrite; Ccp, chalcopyrite; Gn, galena; Sp, sphalerite; Sd, siderite; Mol, molybdenite; Brt, baryte; Ttr, tetrahedrite; Tnt, tennantite; Mnz, monazite; Dol, dolomite; Wtc, wittichenite. BiTe is an abbreviation used to refer to unidentified bismuth tellurides. Sources: (b), (e) and (i) ©National Museums Scotland. Abbreviations are from Warr (2021).

The limitation of representativeness of paragenetic studies is also demonstrated by the relative uncertainty in the placement of Stage 4 in the overall paragenesis (Table 1; Fig. 6). It is possible to state the relative order of Stages 5 and 6 with certainty (because baryte and dolomite are observed to cross-cut monazite and siderite; Fig. 5k and l). Furthermore, given that chalcopyrite veinlets from the Stage 4 mineralization have brecciated tennantite crystals from Stage 3 (Fig. 5j), this relative order is also certain. During petrographic observation, no interactions between Stage 4 and Stage 5 or 6 could be observed. However, it is generally the case that fluids in magmatic–hydrothermal porphyry systems evolve towards a cooler, more carbonate-rich composition over time, meaning that carbonates are typically common in the latter paragenetic stages of the orebody (Sillitoe 2000; Sun *et al.* 2017; Park *et al.* 2021). Ultimately, this interpretation must be treated with caution, until further petrographic observations can confirm the relative order depicted in Figure 6. Although it is clear that molybdenite occurs in cracks within PyA crystals (Fig. 5b and c), and therefore postdates PyA, the relationship between molybdenite and Stage 3 could not be observed directly. However, molybdenite was never observed to display an association with PyC, which is coeval with the inclusion assemblage that is demonstrably later than PyA (Fig. 5); furthermore, molybdenite is commonly observed to precede sulfosalt precipitation in porphyry deposits globally (Berger *et al.* 2008). For this reason, molybdenite has been placed in

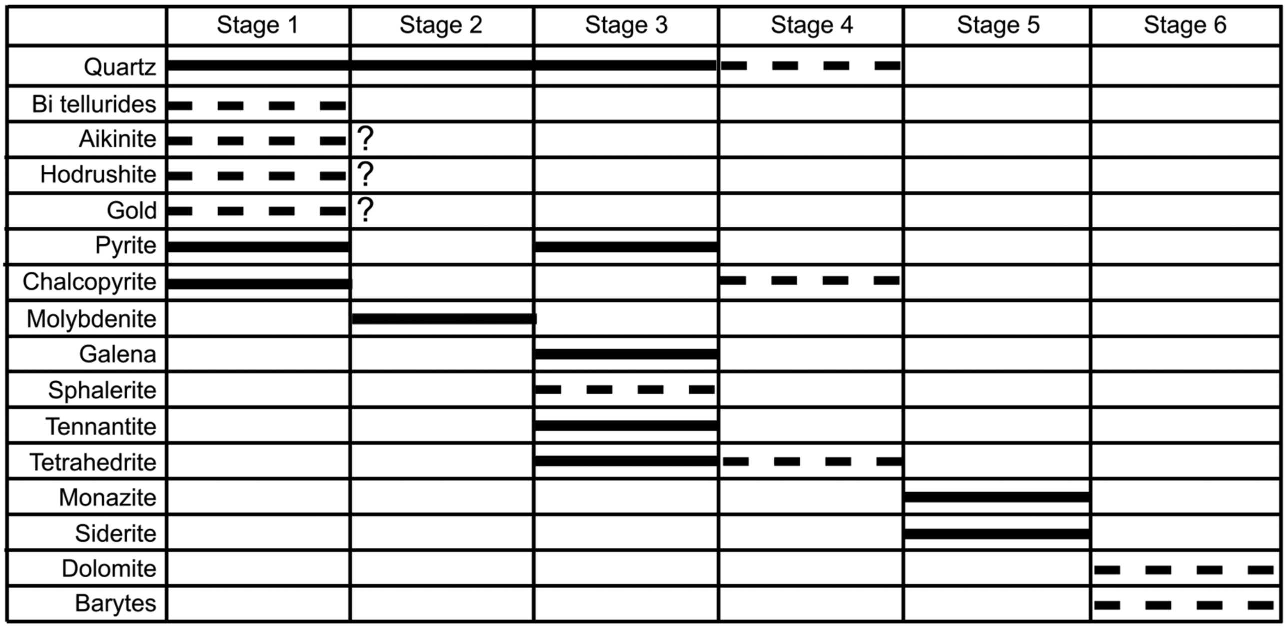


**Fig. 6.** The revised paragenetic interpretation of the Tomnadashan sulfide deposit. Continuous line, major phase; dashed line, minor phase. The question marks represent phases with an uncertain paragenesis (i.e. robust paragenetic relationships could not be established within the present study). Pattrick (1984) described aikinite and hodrushite as being inclusions within the pyrite generation that contains molybdenite and included it as part of the first paragenetic stage. Smith *et al.* (2003) noted that gold occurs as inclusions within pyrite, and in the present study, gold was observed to contain wittichenite inclusions. For these reasons, gold has also been included in Stage 1 of the paragenetic interpretation.

Stage 2, prior to the formation of Stage 3 (Fig. 6). This interpretation is consistent with the paragenetic description by Pattrick (1984), in which galena postdates molybdenite.

Another limitation that is often associated with paragenetic studies is the scale of observation; for example, during petrographic characterization, the field of view may be limited, with the scale bars in Figure 5 usually representing <500 µm. This can sometimes hinder the visualization of paragenetic relationships, and for this reason hand specimens of the mineralization are shown in Figure 4. By considering the mineralogical characteristics at this scale, it is possible to derive additional information that can support the paragenetic interpretation shown in Figure 6; for example, quartz ± carbonate veinlets cross-cutting galena are visible in Figure 4c. It is also clear that pyrite (Fig. 4a) and molybdenite (Fig. 4c) form large volumes of the mineralization at Tomnadashan, providing justification for the decision to classify them as major phases in Figure 6. Considering only the images derived from microscopy would give the misleading impression that molybdenite is a minor phase (Fig. 5b). Finally, the inclusion of a hand specimen of part of the quartz vein at Tomnadashan (Fig. 4d) helps to emphasize that there is a component of vein-hosted mineralization at this locality, which differs mineralogically in some respects (Table 1) from the disseminated mineralization (Fig. 1a).

In this study, we report the first documented occurrence of hydrothermal monazite at Tomnadashan (Fig. 5k; Table 1).

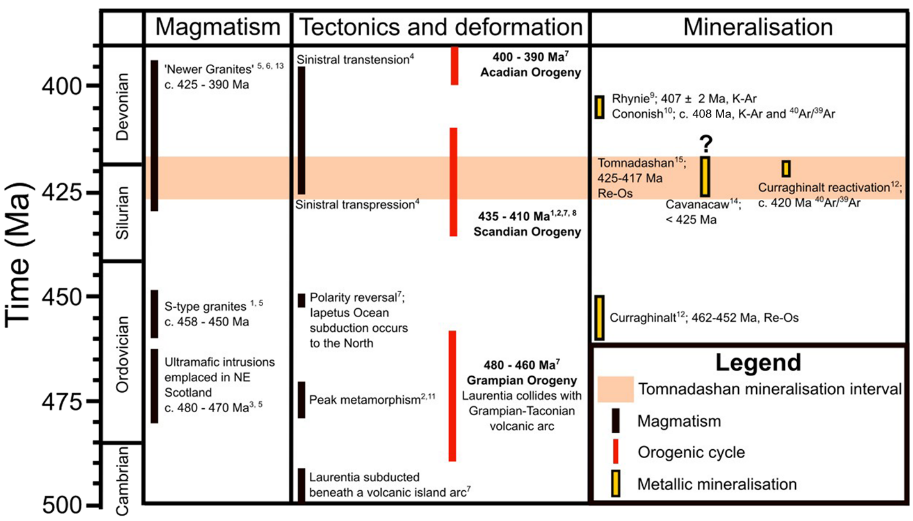


**Fig. 7.** A timeline of tectonic, magmatic, deformation and mineralization events throughout the Grampian Terrane from the Ordovician to the Silurian. The references for the various events are shown as superscript numbers on the timeline. The range for the 'Newer Granites' encompasses the age of the diorite (425 ± 3 Ma) and granite (404 ± 6 Ma) from the Comrie Pluton. The formation of Cavanacaw, an event poorly constained, has been annotated with a question mark. Sources: 1, Jacques and Reavy (1994); 2, Dallmeyer *et al.* (2001); 3, Oliver (2001); 4, Dewey and Strachan (2003); 5, Oliver *et al.* (2008); 6, Neilson *et al.* (2009); 7, Chew and Strachan (2014); 8, Corfu *et al.* (2014); 9, Mark *et al.* (2011); 10, Rice *et al.* (2012); 11, Tanner (2014*a*); 12, Rice *et al.* (2016); 13, Rice *et al.* (2018); 14, Shaw *et al.* (2022); 15, this study. Comrie Pluton ages from Oliver *et al.* (2008).

**Table 2.** Rhenium–osmium data synopsis for molybdenite from the old smelting works around Tomnadashan

| Sample | Weight (g) | Description | Grid reference | Re (ppm) | ± | $^{187}$Re (ppm) | ± | $^{187}$Os (ppb) | ± | Age (Ma) | ±* | ±† | ±‡ |
|---|---|---|---|---|---|---|---|---|---|---|---|---|---|
| TOM_MOLY_SM | 0.106 | Free-growing, vein-hosted molybdenite (Fig. 3a) | NN 687 377 | 123.48 | 0.4 | 77.6 | 0.2 | 548.3 | 1.4 | 422.6 | 0.2 | 1.7 | 2.1 |
| PA_MOLY | 0.051 | Free-growing, vein-hosted molybdenite (Fig. 3b) | NN 68600 37725 | 106.1 | 0.4 | 66.7 | 0.22 | 471.6 | 1.2 | 423.0 | 0.2 | 1.7 | 2.2 |
| G.1878.49.10.1 | 0.021 | Disseminated molybdenite hosted in the granitoid (Fig. 3c) | NN 69125 37914 | 209.9 | 0.8 | 131.9 | 0.5 | 924.0 | 2.9 | 419.0 | 0.3 | 1.7 | 2.1 |

*Uncertainty including only mass spectrometry uncertainty.
†Uncertainty including all sources of analytical uncertainty.
‡Uncertainty including all sources of analytical uncertainty plus decay constant.

Whether it is a primary occurrence, or simply the result of inherited material from the granitoid host rock (in which minerals such as monazite are common), is not completely certain; however, the euhedral morphology, internal zonation and spatial distribution (Fig. 5k) of the monazite appear to demonstrate that these crystals grew from the same fluid that deposited the siderite. The origin of the monazite could be distinguished by further investigations into the Th content of this phase at Tomnadashan, which tends to be much lower in hydrothermal monazite relative to iterations of this phase resulting from magmatic crystallization (Schandl and Gorton 2004). Furthermore, given the preponderance of monazite in carbonatite deposits globally (Chen *et al.* 2017), it is realistic for a carbonic fluid (such as the one evidently responsible in Stage 4 of the Tomnadashan paragenesis) to precipitate this phase.

### Re–Os dating of molybdenite

All molybdenite samples yielded similar dates that overlap (Table 2), with *c.* 2 Ma uncertainty, meaning that the likely mineralization interval of Stage 2 is constrained to between 425 and 417 Ma. Given the fact that molybdenite occurs in one of the earlier paragenetic stages (Fig. 6), prior to the precipitation of the late-stage chalcopyrite veinlets and voluminous carbonate phases (Fig. 6), this would suggest that the Re–Os dates in this study pertain to the initial mineralization event in the Loch Tay mineral system. The ages of these subsequent stages of mineralization (Stage 3 onwards) remain unknown.

There were no significant differences observed in the ages of different forms of molybdenite (disseminated in the granitoid v. hosted in the quartz vein), which further supports the interpretation that the molybdenite collectively belongs to the same paragenetic stage. However, this interpretation is based on three analyses; more data would be needed to state this with absolute certainty.

## Discussion

The Tomnadashan deposit shows both similarities and differences compared with the other Loch Tay veins. Our paragenetic interpretation further demonstrates similarities; for example, at the Glen Almond Vein, there are two distinct pyrite stages and a voluminous carbonate-bearing stage (Webb *et al.* 2024). However, there are many phases that are rarely observed elsewhere, particularly in the eastern part of the Loch Tay area (e.g. bismuth tellurides, tetrahedrite and molybdenite); indeed, Chapman *et al.* (2023) identified two general types of auriferous mineralization in the Loch Tay area: vein-hosted (e.g. Calliachar, Tombuie and Glen Almond) and magmatic–hydrothermal (e.g. Keltie Burn). Based on the mineralogical characteristics described in this study, Tomnadashan appears to have more affinities with the latter.

The Re–Os results (Table 1) represent the first ages for Tomnadashan. The *c.* 423–419 Ma age is older than obtained from other magmatic gold and base metal occurrences in Scotland (*c.* 407 Ma for Cononish, *c.* 408 Ma for Rhynie; Mark *et al.* 2011; Rice *et al.* 2012; Fig. 7). However, the Tomnadashan mineralization age overlaps with the first, dioritic stage of Comrie (425 ± 3 Ma; Oliver *et al.* 2008), although it is unclear whether the arsenopyrite is associated with the diorite or with the later, *c.* 408 Ma granite stage of the pluton; both the granite and diorite subdivisions of Comrie are mineralized (Naden *et al.* 2010). Furthermore, the mineral assemblages recorded by the granite and diorite at Comrie may differ; arsenopyrite, pyrite and chalcopyrite have been described in the diorite, whereas the granite hosts an assemblage of chalcopyrite, pyrite and molybdenite (Naden *et al.* 2010). In addition, the Re–Os ages for Tomnadashan are not dissimilar to those recorded by molybdenite in the Kilmelford Igneous Complex (425.8 ± 1.7 Ma; Conliffe *et al.* 2010).

The obtained age range is compatible with the suggested transition from regional transpression (Fig. 7) to transtension throughout the Grampian Terrane, which facilitated widespread granitoid magmatism across Scotland and similar age granites in Northern Ireland (Jacques and Reavy 1994; Oliver *et al.* 2008; Neilson *et al.* 2009; Cooper *et al.* 2013; Fig. 7). The Tomnadashan age is also compatible with the age, interpreted from structural data, of the Cavanacaw gold–sulfide deposit and other nearby gold-bearing vein occurrences in Northern Ireland (Shaw *et al.* 2022; Fig. 7). The Cavanacaw deposit is not observed to be associated with a magmatic intrusion, but some of the nearby vein occurrences (the Sperrin region veins) have spatial association with a *c.* 425 Ma calc-alkaline intrusive suite (Cooper *et al.* 2013). The dates also overlap with the reactivated fault movements dated at the nearby Curraghinalt deposit (*c.* 424 Ma; Rice *et al.* 2016). Collectively, our data combined with published literature indicate that there were approximately coeval, mid-Silurian, probably magmatic–hydrothermal, gold–base metal mineralization events across the Grampian Terrane from Scotland to Northern Ireland.

Although a magmatic fluid source for Tomnadashan has always been suspected, our collation of previous studies has brought into question the exact source of the ore-forming fluids; the porphyry that crops out at the surface (Fig. 1) is simply the host rock. There may be a further pluton buried near or along the Loch Tay Fault beneath Tomnadashan that was the source of the mineralizing fluids, although without geophysical evidence such suggestions are purely speculative. Alternatively, the granite within the porphyry (Fig. 2b) may also be a viable fluid source, given that the granite corresponds to the development of potassic alteration and is not encompassed within the propylitic halo (Smith 1996); the spatial distribution of hydrothermal alteration at Tomnadashan may suggest that mineralizing fluids migrated away from the granitoids following their emplacement, as is envisioned in the genetic model for Cu–Mo porphyry deposits (Sillitoe 2010). However, more research is needed to better characterize the alteration assemblages at Tomnadashan and identify potential sources of mineralizing fluids. It is also possible that the disseminated mineralization has been overprinted by later mineralization events, potentially during the veining event that is associated with the later paragenetic stages of the orebody (e.g. Stages 3–6 in Fig. 6).

## Conclusions

We have derived the first geochronological age for mineralization around the shores of Loch Tay (*c.* 425–417 Ma). In this study, we have contextualized the age within a refined paragenesis for the mineralization and a comprehensive interpretation of previous studies, and demonstrated the following.

1. Although geochemical evidence clearly implicates a magmatic fluid, mineralization at Tomnadashan is hosted within a fault that postdates the porphyry at the surface. The magmatic fluids were derived from elsewhere, and their exact source is at present unknown.
2. The age possibly coincides with the early stages of regional transtension and the voluminous magmatism at the end of the Caledonian Orogeny.
3. Our data combined with published literature indicate that there were approximately coeval, mid-Silurian, probably magmatic–hydrothermal, gold–base metal mineralization events across the Grampian Terrane from Scotland to Northern Ireland (Fig. 7).

To further bolster the conclusions reached in this study, future work could focus on dating the igneous rocks within the Tomnadashan porphyry itself (e.g. U–Pb dating of zircons) and the various other undated intrusions depicted throughout the study area shown in Figure 1b. Radiometric dates for the granitoids would assist in resolving the relationship between the intrusions and the granitoids; for example, it may be possible to identify an intrusion that is coeval with the molybdenite dates from Tomnadashan. Other potential avenues for future research include the use of sulfur and lead isotopes of the different sulfide minerals at Tomnadashan and the other Loch Tay veins (Fig. 1b), which may provide further constraints on the nature and source of the mineralizing fluids. Furthermore, detailed alteration mapping and petrographical characterization of alteration assemblages could aid in the evaluation of the relationship between the granitoids and the mineralization. This would provide further insight into the potential source of the mineralizing fluids at Tomnadashan (e.g. another concealed pluton, or the granitic dykes within the mine).

*Scientific editing by Iain Neill*

**Acknowledgements** We thank Nature Scotland for giving permission for sampling to take place at Tomnadashan, and National Museums Scotland for providing samples to support this study. The molybdenite used for Re–Os analyses was kindly supplied by S. Moreton, NMS, and P. Aspen. D.S. acknowledges C. Ottley and G. Nowell for laboratory support. We thank Green Glen Minerals for assisting with fieldwork, I. Butler and G. McCay for providing access to polished block TD-0 (Fig. 5j) from the collection of specimens at the University of Edinburgh, and S. Hollis and E. McIntosh for their helpful reviews.

**Author contributions** **SW**: conceptualization (lead), data curation (lead), formal analysis (lead), investigation (equal), visualization (lead), writing – original draft (lead), writing – review & editing (lead); **TT**: conceptualization (equal), data curation (equal), formal analysis (equal), supervision (lead), visualization (equal), writing – review & editing (equal); **RC**: conceptualization (supporting), data curation (supporting), formal analysis (supporting), visualization (supporting), writing – review & editing (supporting); **DS**: data curation (supporting), formal analysis (equal), methodology (equal), visualization (supporting), writing – review & editing (supporting); **RG**: formal analysis (supporting), visualization (supporting), writing – review & editing (supporting)

**Funding** This work was supported by the Leeds–York–Hull National Environment Research Council (NERC) Panorama Doctoral Training Partnership (DTP) under grant NE/2445151.

## Competing interests

The authors declare that they have no known competing financial interests or personal relationships that could have appeared to influence the work reported in this paper.

## Data availability

All data generated or analysed during this study are included in this published article.

## References


Atherton, M.P. and Ghani, A.A. 2002. Slab breakoff: a model for Caledonian, Late Granite syncollisional magmatism in the orthotectonic (metamorphic) zone of Scotland and Donegal, Ireland. *Lithos*, **62**, 65–85, https://doi.org/10.1016/S0024-4937(02)00111-1

Baxter, F.B., Ague, J.J. and DePaolo, D.J. 2002. Prograde temperature–time evolution in the Barrovian type-locality constrained by Sm/Nd garnet ages from Glen Clova, Scotland. *Journal of the Geological Society, London*, **159**, 71–82, https://doi.org/10.1144/0016-76901013

Berger, B., Ayuso, R., Wynn, J. and Seal, R. 2008. *Preliminary Model of Porphyry Copper Deposits*. US Geological Survey Open-File Report, **2008-1321**, https://pubs.usgs.gov/of/2008/1321/pdf/OF081321_508.pdf [last accessed 7 June 2023].

Brown, P., Ryan, P., Soper, N. and Woodcock, N. 2008. The Newer Granite problem revisited: a transtensional origin for the Early Devonian Trans-Suture Suite. *Geological Magazine*, **145**, 235–256, https://doi.org/10.1017/S0016756807004219

Chapman, R.J., Mortensen, J.K., Allan, M.M., Walshaw, R.D., Bond, J. and MacWilliam, K. 2022. A new approach to characterizing deposit type using mineral inclusion assemblages in gold particles. *Economic Geology*, **117**, 361–381, https://doi.org/10.5382/econgeo.4863

Chapman, R.J., Torvela, T. and Savastano, L. 2023. Insights into regional metallogeny from detailed compositional studies of alluvial gold: an example from the Loch Tay area, Central Scotland. *Minerals*, **13**, https://doi.org/10.3390/min13020140

Chen, W., Huang, H., Bai, T. and Jiang, S. 2017. Geochemistry of monazite within carbonatite related REE deposits. *Resources*, **6**, 51, https://doi.org/10.3390/resources6040051

Chew, D. and Strachan, R. 2014. The Laurentian Caledonides of Scotland and Ireland. *Geological Society, London, Special Publications*, **390**, 45–91, https://doi.org/10.1144/SP390.16

Conliffe, J., Selby, D., Porter, S. and Feely, M. 2010. Re–Os molybdenite dates from the Ballachulish and Kilmelford Igneous Complexes (Scottish Highlands): age constraints for late Caledonian magmatism. *Journal of the Geological Society, London*, **167**, 297–302, https://doi.org/10.1144/0016-76492009-077

Cooper, M., Crowley, Q. *et al.* 2011. Age constraints and geochemistry of the Ordovician Tyrone Igneous Complex, Northern Ireland: implications for the Grampian orogeny. *Journal of the Geological Society, London*, **168**, 837–850, https://doi.org/10.1144/0016-76492010-164

Cooper, M.R., Crowley, Q.G., Hollis, S.P., Noble, S.R. and Henney, P.J. 2013. A U–Pb age for the Late Caledonian Sperrin Mountains minor intrusions suite in the north of Ireland: timing of slab break-off in the Grampian terrane and the significance of deep-seated, crustal lineaments. *Journal of the Geological Society, London*, **170**, 603–614, https://doi.org/10.1144/jgs2012-098

Corfu, F., Gasser, D. and Chew, D.M. 2014. New perspectives on the Caledonides of Scandinavia and related areas: introduction. *Geological Society, London, Special Publications*, **390**, 1–8, https://doi.org/10.1144/SP390.28

Corkhill, C., Ixer, R., Mason, J., Irving, D. and Pattrick, R. 2010. Polymetallic auriferous vein mineralization near Loch Tay, Perthshire, Scotland. *Scottish Journal of Geology*, **46**, 23–30, https://doi.org/10.1144/0036-9276/01-378

Creaser, R.A., Papanastassiou, D.A. and Wasserburg, G.J. 1991. Negative thermal ion mass-spectrometry of osmium, rhenium, and iridium. *Geochimica et Cosmochimica Acta*, **55**, 397–401, https://doi.org/10.1016/0016-7037(91)90427-7

Dallmeyer, R.D., Strachan, R.A., Rogers, G., Watt, G.R. and Friend, C.R.L. 2001. Dating deformation and cooling in the Caledonian thrust nappes of north Sutherland, Scotland: insights from $^{40}Ar/^{39}Ar$ and Rb–Sr chronology. *Journal of the Geological Society, London*, **158**, 501–512, https://doi.org/10.1144/jgs.158.3.501

Dempster, T. 1985. Uplift patterns and orogenic evolution in the Scottish Dalradian. *Journal of the Geological Society, London*, **142**, 111–128, https://doi.org/10.1144/gsjgs.142.1.0111

Dempster, T.J., Hudson, N.F.C. and Rogers, G. 1995. Metamorphism and cooling of the NE Dalradian. *Journal of the Geological Society, London*, **152**, 383–390, https://doi.org/10.1144/gsjgs.152.2.0383

Devéria, R. 2001. Tomnadashan: a re-examination of a nineteenth century copper mining and smelting operation in Perthshire, Scotland. *Historical Metallurgy*, **35**, 87–98.

Dewey, J. 2005. Orogeny can be very short. *Proceedings of the National Academy of Sciences of the USA*, **102**, 15286–15293, https://doi.org/10.1073/pnas.0505516102

Dewey, J. and Mange, M. 1999. Petrography of Ordovician and Silurian sediments in the western Irish Caledonides: tracers of a short-lived Ordovician continent–arc collision orogeny and the evolution of the Laurentian Appalachian–Caledonian margin. *Geological Society, London, Special Publications*, **164**, 55–107, https://doi.org/10.1144/GSL.SP.1999.164.01.05

Dewey, J.F. and Strachan, R.A. 2003. Changing Silurian–Devonian relative plate motion in the Caledonides; sinistral transpression to sinistral transtension. *Journal of the Geological Society, London*, **160**, 219–229, https://doi.org/10.1144/0016-764902-085

Freeman, B., Klemperer, S.L. and Hobbs, R.W. 1988. The deep structure of northern England and the Iapetus Suture zone from BIRPS deep seismic reflection profiles. *Journal of the Geological Society, London*, **145**, 727–740, https://doi.org/10.1144/gsjgs.145.5.0727

Friedrich, A.M., Bowring, S.A., Martin, M.W. and Hodges, K.V. 1999. Short-lived continental magmatic arc at Connemara, western Ireland Caledonides: implications for the age of the Grampian orogeny. *Geology*, **27**, 27–30, https://doi.org/10.1130/0091-7613(1999)027<0027:SLCMAA>2.3.CO;2

Goldfarb, R. and Groves, D. 2015. Orogenic gold: common or evolving fluid and metal sources through time. *Lithos*, **233**, 2–26, https://doi.org/10.1016/j.lithos.2015.07.011

Goldfarb, R.J. and Pitcairn, I. 2022. Orogenic gold: is a genetic association with magmatism realistic? *Mineralium Deposita*, **58**, 5–35, https://doi.org/10.1007/s00126-022-01146-8

Gramlich, J.W., Murphy, T.J., Garner, E.L. and Shields, W.R. 1973. Absolute isotopic abundance ratio and atomic weight of a reference sample of rhenium. *Journal of Research of the National Institute of Standards and Technology*, **77**, 691–698.

Halliday, L.B. 1961. *Loch Tay Copper - Scotland*. Toronto Geologist's Report, Project **389** [issued 4 December 1961].

Henwood, W.J. 1871. Notes on the molybdenite of Tomnadashan in Perthshire. *Transactions of the Royal Geological Society of Cornwall*, **8**, 650–654.

Hines, R., Paterson, S.R., Memeti, V. and Chambers, J.A. 2018. Nested incremental growth of zoned upper crustal plutons in the Southern Uplands Terrane, UK: fractionating, mixing, and contaminated magma fingers. *Journal of Petrology*, **59**, 483–516, https://doi.org/10.1093/petrology/egy034

Holmes, A. 1946. An estimate of the age of the earth. *Nature*, **157**, 680–684, https://doi.org/10.1038/157680a0

Huston, D.L. and Champion, D.C. 2023. Applications of lead isotopes to ore geology, metallogenesis and exploration. *In*: Huston, D. and Gutzmer, J. (eds) *Isotopes in Economic Geology, Metallogenesis and Exploration*. Mineral Resource Reviews. Springer, Cham, 155–187.

Ixer, R., Pattrick, R. and Stanley, C. 1997. Geology, mineralogy and genesis of gold mineralization at Calliachar–Urlar Burn, Scotland. *Transactions of the Institution of Mining and Metallurgy, Section B*, **106**, 99–108.

Jacques, J.M. and Reavy, R.J. 1994. Caledonian plutonism and major lineaments in the SW Scottish Highlands. *Journal of the Geological Society, London*, **151**, 955–969, https://doi.org/10.1144/gsjgs.151.6.0955

Lawley, C. and Selby, D. 2012. Re–Os geochronology of quartz-enclosed ultrafine molybdenite: implications for ore geochronology. *Economic Geology*, **107**, 1499–1505, https://doi.org/10.2113/econgeo.107.7.1499

Li, Y., Selby, D., Condon, D. and Tapster, S. 2017. Cyclic magmatic–hydrothermal evolution in porphyry systems: high-precision U–Pb and Re–Os geochronology constraints on the Tibetan Qulong Porphyry Cu–Mo deposit. *Economic Geology*, **112**, 1419–1440, https://doi.org/10.5382/econgeo.2017.4515

Lowry, D., Boyce, A.J., Fallick, A.E., Stephens, W.E. and Grassineau, N.V. 2005. Terrane and basement discrimination in northern Britain using sulphur isotopes and mineralogy of ore deposits. *Geological Society, London, Special Publications*, **248**, 131–151, https://doi.org/10.1144/GSL.SP.2005.248.01.07

Mark, D., Rice, C., Fallick, A., Trewin, N., Lee, M., Boyce, A. and Lee, J. 2011. $^{40}Ar/^{39}Ar$ dating of hydrothermal activity, biota and gold mineralization in the Rhynie hot-spring system, Aberdeenshire, Scotland. *Geochimica et Cosmochimica Acta*, **75**, 555–569, https://doi.org/10.1016/j.gca.2010.10.014

Mark, D.F., Rice, C.M., Hole, M. and Condon, D. 2020. Multi-chronometer dating of the Souter Head complex: rapid exhumation terminates the Grampian Event of the Caledonian Orogeny. *Earth and Environmental Science Transactions of the Royal Society of Edinburgh*, **11**, 1–14, https://doi.org/10.1017/S1755691020000043

McKerracher, A. 1988. *Perthshire in History and Legend*. John Donald, Edinburgh.

Mendum, J.R. and Noble, S.R. 2010. Mid-Devonian sinistral transpression on the Great Glen Fault: the rise of the Rosemarkie Inlier and the Acadian Event in Scotland. *Geological Society, London, Special Publications*, **335**, 161–187, https://doi.org/10.1144/SP.335.8

Miles, A., Graham, C., Hawkesworth, C., Gillespie, M., Dhuime, B. and Hinton, R. 2014. Using zircon isotope compositions to constrain crustal structure and pluton evolution: the Iapetus Suture Zone granites in Northern Britain. *Journal of Petrology*, **55**, 181–207, https://doi.org/10.1093/petrology/egt065

Miles, A.J., Woodcock, N.H. and Hawkesworth, C.J. 2016. Tectonic controls on post-subduction granite genesis and emplacement: the late Caledonian suite of Britain and Ireland. *Gondwana Research*, **39**, 250–260, https://doi.org/10.1016/j.gr.2016.02.006

MI-SWACO 2014. *Duntanlich Mine Plan*. Presentation prepared by Dalgleish Associates Limited, Dunblane.

Moles, N. and Selby, D. 2023. Implications of new geochronological constraints on the Aberfeldy stratiform barite deposits, Scotland, for the depositional continuity and global correlation of the Neoproterozoic Dalradian Supergroup.

*Precambrian Research*, **384**, 106925, https://doi.org/10.1016/j.precamres.2022.106925

Moles, N., Boyce, A. and Fallick, A. 2014. Abundant sulphate in the Neoproterozoic ocean: implications of constant $\delta^{34}S$ of barite in the Aberfeldy SEDEX deposits, Scottish Dalradian. *Geological Society, London, Special Publications*, **393**, 189–212, https://doi.org/10.1144/SP393.7

Moorbath, S. 1962. Lead isotope abundance studies on mineral occurrences in the British Isles and their geological significance. *Philosophical Transactions of the Royal Society of London, Series A*, **254**, 295–360.

Naden, J., Gunn, A.G. and Shephard, T.J. 2010. *Fluids and Mineralisation in the Scottish Dalradian*. British Geological Survey Internal Report, **OR/09/054**.

Neilson, J.C., Kokelaar, B.P. and Crowley, Q.G. 2009. Timing, relations and cause of plutonic and volcanic activity of the Siluro-Devonian post-collision magmatic episode in the Grampian Terrane, Scotland. *Journal of the Geological Society, London*, **166**, 545–561, https://doi.org/10.1144/0016-76492008-069

Nier, A.O. 1950. A redetermination of the relative abundances of the isotopes of carbon, nitrogen, oxygen, argon, and potassium. *Physical Review*, **77**, 789, https://doi.org/10.1103/PhysRev.77.789

Oliver, G.J.H. 2001. Reconstruction of the Grampian episode in Scotland: its place in the Caledonian Orogeny. *Tectonophysics*, **332**, 23–49, https://doi.org/10.1016/S0040-1951(00)00248-1

Oliver, G., Wilde, S. and Wan, Y. 2008. Geochronology and geodynamics of Scottish granitoids from the late Neoproterozoic break-up of Rodinia to Palaeozoic collision. *Journal of the Geological Society, London*, **165**, 661–674, https://doi.org/10.1144/0016-76492007-105

O'Reilly, B.M., Hauser, F. and Readman, P.W. 2012. The fine-scale seismic structure of the upper lithosphere within accreted Caledonian lithosphere: implications for the origins of the 'Newer Granites'. *Journal of the Geological Society, London*, **169**, 561–573, https://doi.org/10.1144/0016-76492011-128

Park, J.-W., Campbell, I.H., Chiaradia, M., Hao, H. and Lee, C.-T. 2021. Crustal magmatic controls on the formation of porphyry copper deposits. *Nature Reviews Earth & Environment*, **2**, 542–557, https://doi.org/10.1038/s43017-021-00182-8

Parnell, J., Earls, G. *et al.* 2000. Regional fluid flow and gold mineralization in the Dalradian of the Sperrin Mountains, Northern Ireland. *Economic Geology*, **95**, 1389–1416, https://doi.org/10.2113/gsecongeo.95.7.1389

Pattrick, R. 1984. Sulphide mineralogy of the Tomnadashan copper deposit and the Corrie Buie lead veins, south Loch Tayside, Scotland. *Mineralogical Magazine*, **48**, 85–91, https://doi.org/10.1180/minmag.1984.048.346.11

Phillips, G. and Powell, R. 2010. Formation of gold deposits: a metamorphic devolatilization model. *Journal of Metamorphic Geology*, **28**, 689–718, https://doi.org/10.1111/j.1525-1314.2010.00887.x

Porter, S. and Selby, D. 2010. Rhenium–osmium (Re–Os) molybdenite systematics and geochronology of the Cruachan Granite skarn mineralization, Etive Complex: implications for emplacement chronology. *Scottish Journal of Geology*, **46**, 17–21, https://doi.org/10.1144/0036-9276/01-398

Rice, C., Mark, D., Selby, D. and Hill, N. 2012. Dating vein-hosted Au deposits in the Caledonides of N. Britain. *Transactions of the Institute of Mining and Metallurgy, Section B*, **121**, 199–200.

Rice, C., Mark, D., Selby, D., Neilson, J. and Davidheiser-Kroll, B. 2016. Age and geologic setting of quartz vein-hosted gold mineralization at Curraghinalt, Northern Ireland: implications for genesis and classification. *Economic Geology*, **111**, 127–150, https://doi.org/10.2113/econgeo.111.1.127

Rice, S., Cuthbert, S. and Hursthouse, A. 2018. Tectono-magmatic controls of post-subduction gold mineralisation during late Caledonian soft continental collision in the Southern Uplands–Down–Longford Terrane, Britain and Ireland: a review. *Ore Geology Reviews*, **101**, 74–104, https://doi.org/10.1016/j.oregeorev.2018.07.016

Roberts, J.L. and Treagus, J.E. 1977. Polyphase generation of nappe structures in the Dalradian rocks of the southwest Highlands of Scotland. *Scottish Journal of Geology*, **13**, 237–254, https://doi.org/10.1144/sjg13030237

Schandl, E.S. and Gorton, M.P. 2004. A textural and geochemical guide to the identification of hydrothermal monazite: criteria for selection of samples for dating epigenetic hydrothermal ore deposits. *Economic Geology*, **99**, 1027–1035, https://doi.org/10.2113/gsecongeo.99.5.1027

Scotgold Resources Limited 2015. Cononish gold project study update and JORC 2012 ore reserve estimate, https://announcements.asx.com.au/asxpdf/20150526/pdf/42yt26kn3xqj6x.pdf

Searle, M.P. 2022. Tectonic evolution of the Caledonian orogeny in Scotland: a review based on the timing of magmatism, metamorphism and deformation. *Geological Magazine*, **159**, 124–152, https://doi.org/10.1017/S0016756821000947

Selby, D. and Creaser, R. 2001. Re–Os geochronology and systematics in molybdenite from the Endako porphyry molybdenum deposit, British Columbia, Canada. *Economic Geology*, **96**, 197–204, https://doi.org/10.2113/gsecongeo.96.1.197

Selby, D. and Creaser, R.A. 2004. Macroscale NTIMS and microscale LA-MC-ICP-MS Re–Os isotopic analysis of molybdenite: testing spatial restrictions for reliable Re–Os age determinations, and implications for the decoupling of Re and Os within molybdenite. *Geochimica et Cosmochimica Acta*, **68**, 3897–3908, https://doi.org/10.1016/j.gca.2004.03.022

Selby, D., Creaser, R.A. and Feely, M. 2004. Accurate and precise Re–Os molybdenite dates from the Galway Granite, Ireland. Critical comment on 'Disturbance of the Re–Os chronometer of molybdenites from the late-Caledonian Galway Granite, Ireland, by hydrothermal fluid circulation' by Suzuki *et al.*, *Geochemical Journal*, **35**, pp.29–35, 2001. *Geochemical Journal*, **38**, 291–294, https://doi.org/10.2343/geochemj.38.291

Shaw, J. 2023. *Integration of local and regional structural data with gold microchemistry in the Sperrin Mountains of Northern Ireland and implications for regional exploration models*. PhD thesis, University of Leeds.

Shaw, J., Torvela, T., Cooper, M.R., Leslie, G. and Chapman, R. 2022. A progressive model for the development of the Cavanacaw Au–Ag–Pb vein deposit, Northern Ireland, and implications for the evolution and metallogeny of the Grampian Terrane. *Journal of Structural Geology*, **161**, 104637, https://doi.org/10.1016/j.jsg.2022.104637

Shirey, S.B. and Walker, R.J. 1995. Carius tube digestion for low-blank rhenium–osmium analysis. *Analytical Chemistry*, **67**, 2136–2141, https://doi.org/10.1021/ac00109a036

Sillitoe, R. 2000. Gold-rich porphyry deposits. *In*: Hagemann, G. and Brown, P. (eds) *Gold in 2000*. Society of Economic Geologists, Boulder, CO, 315–345.

Sillitoe, R.H. 2010. Porphyry copper systems. *Economic Geology*, **105**, 3–41, https://doi.org/10.2113/gsecongeo.105.1.3

Smith, C.G., Gunn, A.G., Shepherd, T.J., Coats, J.S. and Wiggans, G.N. 2003. *Gold in the Dalradian Terrane: A Review of Previous Work*. BGS Internal Report, **IR/03/158**.

Smith, C.G., Livingstone, A. and Highton, A.J. 2022. Scottish mineral geological conservation review sites – magmatic and skarn minerals. *Proceedings of the Geologists' Association*, **133**, 350–366, https://doi.org/10.1016/j.pgeola.2019.10.006

Smith, D.G. 1996. *Fractures and mineralisation in the Scottish Dalradian*. PhD thesis, University of Manchester.

Smoliar, M., Walker, R. and Morgan, J. 1996. Re–Os ages of group IIA, IIIA, IVA, and IVB iron meteorites. *Science*, **271**, 1099–1102, https://doi.org/10.1126/science.271.5252.1099

Soper, N.J., Ryan, P.D. and Dewey, J.F. 1999. Age of the Grampian Orogeny in Scotland and Ireland. *Journal of the Geological Society, London*, **156**, 1231–1236, https://doi.org/10.1144/gsjgs.156.6.1231

Spence-Jones, C.P., Jenkin, G.R.T., Boyce, A.J., Hill, N.J. and Sangster, C.J.S. 2018. Tellurium, magmatic fluids and orogenic gold: an early magmatic fluid pulse at Cononish Gold Deposit, Scotland. *Ore Geology Reviews*, **102**, 894–905, https://doi.org/10.1016/j.oregeorev.2018.05.014

Stein, H., Markey, R., Morgan, J., Hannah, J. and Schersten, A. 2001. The remarkable Re–Os chronometer in molybdenite: how and why it works. *Terra Nova*, **13**, 479–486, https://doi.org/10.1046/j.1365-3121.2001.00395.x

Stephenson, D., Mendum, J., Fettes, D. and Leslie, A. 2013. The Dalradian rocks of Scotland: an introduction. *Proceedings of the Geologists' Association*, **124**, 3–82, https://doi.org/10.1016/j.pgeola.2012.06.002

Sun, W., Wang, J. *et al.* 2017. The formation of porphyry copper deposits. *Acta Geochimica*, **36**, 9–15, https://doi.org/10.1007/s11631-016-0132-4

Tanner, P.W.G. 2014*a*. A kinematic model for the Grampian Orogeny, Scotland. *Geological Society, London, Special Publications*, **390**, 467–511, https://doi.org/10.1144/SP390.23

Tanner, P. 2014*b*. Structural controls and origin of gold–silver mineralization in the Grampian Terrane of Scotland and Ireland. *Geological Magazine*, **151**, 1072–1094, https://doi.org/10.1017/S0016756813001131

Treagus, J. 2003. The Loch Tay Fault: type section geometry and kinematics. *Scottish Journal of Geology*, **39**, 135–144, https://doi.org/10.1144/sjg39020135

Treagus, J.E., Pattrick, R.A.D. and Curtis, S.F. 1999. Movement and mineralization in the Tyndrum fault zone, Scotland and its regional significance. *Journal of the Geological Society, London*, **156**, 591–604, https://doi.org/10.1144/gsjgs.156.3.0591

Völkening, J., Walczyk, T. and Heumann, K.G. 1991. Osmium isotope ratio determinations by negative thermal ionization mass spectrometry. *International Journal of Mass Spectrometry and Ion Processes*, **105**, 147–159, https://doi.org/10.1016/0168-1176(91)80077-Z

Warr, L.N. 2021. IMA–CNMNC approved mineral symbols. *Mineralogical Magazine*, **85**, 291–320, https://doi.org/10.1180/mgm.2021.43

Webb, S., Torvela, T., Chapman, R. and Savastano, L. 2024. Textural mapping and building a paragenetic interpretation of hydrothermal veins. *Geological Society, London, Special Publications*, **541**, https://doi.org/10.1144/SP541-2023-17

Zartman, R.E. and Doe, B.R. 1981. Plumbotectonics – the model. *Tectonophysics*, **75**, 135–162, https://doi.org/10.1016/0040-1951(81)90213-4